

# Thermal model description of $p$ - $Pb$ collisions at $\sqrt{s_{NN}} = 5.02$ TeV

Natasha Sharma<sup>1,a</sup>, Jean Cleymans<sup>2,b</sup>, Lokesh Kumar<sup>1,c</sup>

<sup>1</sup> Department of Physics, Panjab University, Chandigarh 160014, India

<sup>2</sup> UCT-CERN Research Centre and Department of Physics, University of Cape Town, Rondebosch 7701, South Africa

Received: 26 February 2018 / Accepted: 26 March 2018 / Published online: 9 April 2018

© The Author(s) 2018

**Abstract** The ALICE data on light flavor hadron production obtained in  $p$ - $Pb$  collisions at  $\sqrt{s_{NN}} = 5.02$  TeV are studied in the thermal model using the canonical approach with exact strangeness conservation. The chemical freeze-out temperature is independent of centrality except for the lowest multiplicity bin, with values close to 160 MeV but consistent with those obtained in  $Pb$ - $Pb$  collisions at  $\sqrt{s_{NN}} = 2.76$  TeV. The value of the strangeness non-equilibrium factor  $\gamma_s$  is slowly increasing with multiplicity from 0.9 to 0.96, i.e. it is always very close to full chemical equilibrium.

## 1 Introduction

Over the last three decades, the hadron resonance gas (thermal model for short) in its grand-canonical (GC) and canonical formulations has been very successful in describing the abundances of light flavored hadron obtained in heavy-ion collisions [1–3] up to the highest beam energies.

The thermal model has a long history going back to papers by Heisenberg [4], Fermi [5] and Hagedorn [6]. The model uses a minimal number of parameters, mainly, the chemical freeze-out temperature  $T_{ch}$ , the baryon chemical potential  $\mu_B$  and the volume  $V$ . The physical description emerging from this is a very consistent one, the freeze-out temperature rises rapidly at low beam energies to reach a plateau at around 160 MeV while the baryon-chemical potential decreases steadily from a very high value to become compatible with zero at the highest energies. The implication is that all hadrons are produced at one temperature and within one volume. It is therefore of interest to test the region of applicability of the

thermal model and this is done in the present paper for  $p$ - $Pb$  collisions at the LHC.

In the present paper we investigate in detail the particle abundances in  $p$ - $Pb$  collisions [7–10] in the hope that this contributes to the understanding and the status of the model description.

At LHC energies, the particle abundances in central heavy-ion collisions have been well described [3, 11, 12] over nine orders of magnitude with only two parameters  $T_{ch}$  and  $V$ , with  $\mu_B$  being restricted to zero because of the particle-antiparticle symmetry at the LHC.

Our results show that there is no clear dependence on the centrality, as measured by the values of  $dN_{ch}/d\eta$ , for the chemical freeze-out temperature. This confirms results obtained earlier on the dependence of thermal parameters on the size of the system obtained [13].

In Sect. 2 we briefly review the main features of the model. Section 3 presents our results for  $p$ - $Pb$  collisions. Section 4 contains a discussion of results and Sect. 5 presents our conclusions.

## 2 The model

The identifying feature of the thermal model is that all the resonances listed in [14] are assumed to be in thermal and chemical equilibrium. This assumption drastically reduces the number of free parameters as this stage is determined by just a few thermodynamic variables namely, the chemical freeze-out temperature  $T_{ch}$ , the various chemical potentials  $\mu$  determined by the conserved quantum numbers and by the volume  $V$  of the system. It has been shown that this description is also the correct one [15–17] for a scaling expansion as first discussed by Bjorken [18]. After integration over  $pT$  these authors have shown that:

$$\frac{dN_i/dy}{dN_j/dy} = \frac{N_i^0}{N_j^0} \quad (1)$$

In memory of Helmut Oeschler.

<sup>a</sup> e-mail: natasha.sharma@cern.ch

<sup>b</sup> e-mail: jean.cleymans@uct.ac.za

<sup>c</sup> e-mail: kumar.lokesh@cern.ch

where  $N_i^0$  is the particle yield as calculated in a fireball at rest. Hence, in the Bjorken model with longitudinal scaling and radial expansion the effects of hydrodynamic flow cancel out in ratios.

In general, if the number of particles carrying quantum numbers related to a conservation law is small, then the grand-canonical description no longer holds. In such a case the conservation of quantum numbers has to be implemented exactly in the canonical ensemble [19,20]. Here, we refer only to strangeness conservation and consider charge and baryon number conservation to be fulfilled on the average in the grand canonical ensemble because the number of charged particles and baryons is much larger than that of strange particles [21].

In the *Grand-Canonical Ensemble (GCE)*, the volume  $V$ , temperature  $T_{ch}$  and the chemical potentials  $\vec{\mu}$  determine the partition function  $Z(T, V, \vec{\mu})$ . In the hadronic fireball of non-interacting hadrons,  $\ln Z$  is the sum of the contributions of all  $i$ -particle species

$$\frac{1}{V} \ln Z(T, V, \vec{\mu}) = \sum_i Z_i^1(T, \vec{\mu}), \tag{2}$$

where  $\vec{\mu} = (\mu_B, \mu_S, \mu_Q)$  are the chemical potentials related to the conservation of baryon number, strangeness and electric charge, respectively.  $Z_i^1$  is the one-particle partition function.

The partition function contains all information needed to obtain the number density  $n_i$  of particle species  $i$ . Introducing the particle's specific chemical potential  $\mu_i$ , one gets

$$n_i(T, \vec{\mu}) = \frac{1}{V} \left. \frac{\partial(T \ln Z)}{\partial \mu_i} \right|_{\mu_i=0}. \tag{3}$$

Any resonance that decays into species  $i$  contributes to the yields eventually measured. Therefore, the contributions from all heavier hadrons that decay to hadron  $i$  are included.

In the GCE the particle yields are determined by the volume of the fireball, its temperature and the chemical potentials.

If the number of particles is small, conservation laws have to be implemented exactly. We refer here only to the *Strangeness Canonical Ensemble (SCE)* in which strangeness conservation is considered and charge and baryon number are conserved on the average. The density of strange particle  $i$  carrying strangeness  $s$  can be obtained from [21],

$$n_i^C = \frac{Z_i^1}{Z_{S=0}^C} \sum_{k=-\infty}^{\infty} \sum_{p=-\infty}^{\infty} a_3^p a_2^k a_1^{-2k-3p-s} I_k(x_2) I_p(x_3) I_{-2k-3p-s}(x_1), \tag{4}$$

where  $Z_{S=0}^C$  is the canonical partition function

$$Z_{S=0}^C = e^{S_0} \sum_{k=-\infty}^{\infty} \sum_{p=-\infty}^{\infty} a_3^p a_2^k a_1^{-2k-3p} I_k(x_2) I_p(x_3) I_{-2k-3p}(x_1),$$

where  $Z_i^1$  is the one-particle partition function calculated for  $\mu_S = 0$  in the Boltzmann approximation. The arguments of the Bessel functions  $I_s(x)$  and the parameters  $a_i$  are introduced as,

$$a_s = \sqrt{S_s/S_{-s}}, \quad x_s = 2V\sqrt{S_s S_{-s}}, \tag{5}$$

where  $S_s$  is the sum of all  $Z_k^1(\mu_S = 0)$  for particle species  $k$  carrying strangeness  $s$ .

In the limit where  $x_n < 1$  (for  $n = 1, 2$  and  $3$ ) the density of strange particles carrying strangeness  $s$  is well approximated by [21]

$$\frac{n_i^{SCE}}{n_i^{GCE}} \simeq \frac{I_s(x_1)}{I_0(x_1)}. \tag{6}$$

From these equations it is clear that in the canonical ensemble the strange particle density depends explicitly on the volume through the arguments of the Bessel functions. It has been suggested that this volume might be different from the overall volume  $V$  [22,23]. In our analysis we will not entertain this possibility and work instead with an overall parameter  $\gamma_s$  to describe the deviation of strange particles from chemical equilibrium [24]. This amounts to replacing each particle density by

$$n_i^C \rightarrow \gamma_s^{|s|} n_i^C \tag{7}$$

where  $|s|$  is the sum of the number of strange and anti-strange quarks. Note that the  $\phi$  meson picks up a factor  $\gamma_s^2$  since it contains a strange and an anti-strange quark. This makes the  $\phi$  meson behave in a similar way to the  $\Xi$  baryon which contains two strange quarks, a behavior which is supported by the data. The changes for the other strange mesons and baryons are as follows:

$$\begin{aligned} n_K^C &\rightarrow \gamma_s n_K^C, \\ n_\Lambda^C &\rightarrow \gamma_s n_\Lambda^C, \\ n_\Xi^C &\rightarrow \gamma_s^2 n_\Xi^C, \\ n_\Omega^C &\rightarrow \gamma_s^3 n_\Omega^C. \end{aligned}$$

### 3 Scaling of yields with strange quark content

The experimental results were taken from [7–9], these are obtained for central rapidity in an interval  $\Delta y = 1$ . One of the basic features of the SC approach is that the particle ratios exhibit an approximate scaling with the difference

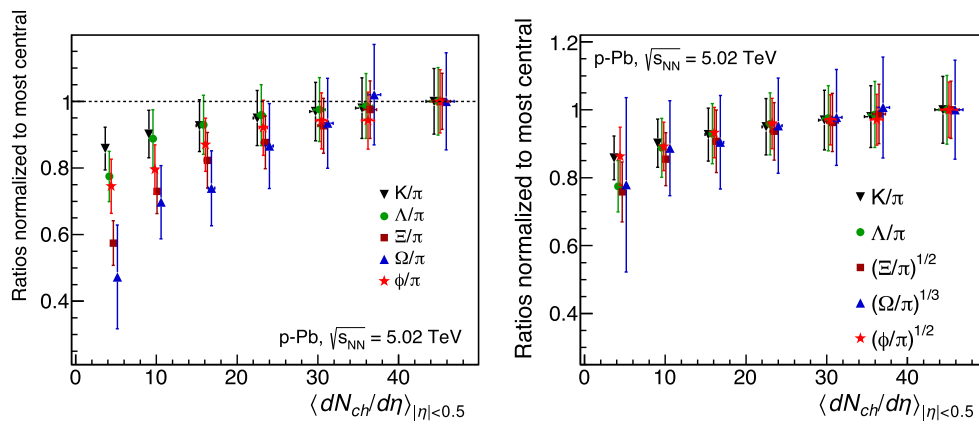


**Fig. 1** The ratios of strange particle yields to pion yields, normalized to the corresponding value at the highest multiplicity, as a function of  $\langle dN_{ch}/d\eta \rangle_{|\eta|<0.5}$  for  $p$ - $Pb$  collisions at 5.02 TeV, left as measured, right scaled with a power determined by the number of strange and antistrange quarks in the hadron

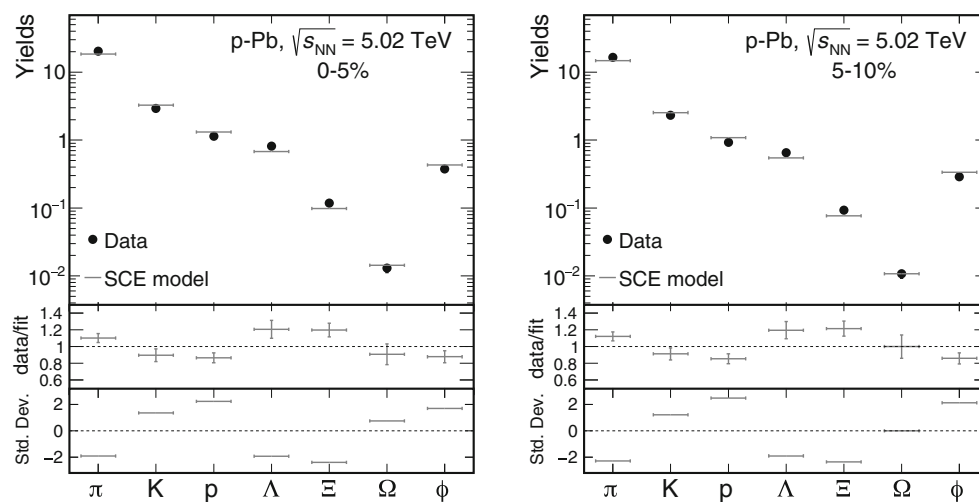


**Fig. 2** Comparison of data with fits for the two most central bins

of the strangeness quantum numbers. The support for this scaling is shown in Fig. 1. The left pane shows the ratios of various strange particle to pion yields  $i$  as a function of multiplicity. Following references [7–9] we use  $K/\pi$  as an abbreviation for the ratio  $(K^+ + K^-)/(\pi^+ + \pi^-)$  and similarly for all other ratios, except that  $\phi/\pi$  is an abbreviation for  $\phi/(\pi^+ + \pi^-)/2$ . Scaling these ratios with the power of the corresponding number of strange quarks one observes a common trend (right pane of Fig. 1). As can be seen from Fig. 1 scaling with the number of strange quarks is very well supported by the experimental data.

This scaling behavior with strange quark content is motivated by the SCE description including the factor  $\gamma_s$ . In particular, the yield of  $\phi$  mesons closely follows the one of e.g.  $\Xi$  baryons. This argues against the use of a different correlation radius for the strangeness suppression as this would not affect the  $\phi$  meson since it has strangeness zero.

#### 4 Fits using the thermal model

In this section we present fits to the hadronic yields obtained in  $p$ - $Pb$  collisions at  $\sqrt{s_{NN}} = 5.02$  TeV in seven multiplicity bins such as 0–5, 10–20, 20–40, 40–60, 60–80 and 80–100%.

We have used THERMUS [25] to perform these fits in the strangeness canonical ensemble (SCE) with  $\mu_B$  and  $\mu_Q$  fixed to 0 and using only one radius  $R$  for the system. The fits to the bins with the most central collisions are shown in Fig. 2. In the following figures  $\pi$  refers to  $(\pi^+ + \pi^-)/2$ ,  $K$  refers to  $(K^+ + K^-)/2$  and similarly  $p$  refers to  $(p + \bar{p})/2$ ,  $\Lambda$  refers to  $(\Lambda + \bar{\Lambda})/2$ ,  $\Xi$  refers to  $(\Xi^- + \bar{\Xi})/2$  and finally  $\Omega$  refers to  $(\Omega + \bar{\Omega})/2$ . All fits were performed including the  $\phi$  meson.

The upper part of the figures compares the experimental results, shown as a black circle, to the fits obtained from the thermal model as described in the previous section. As the

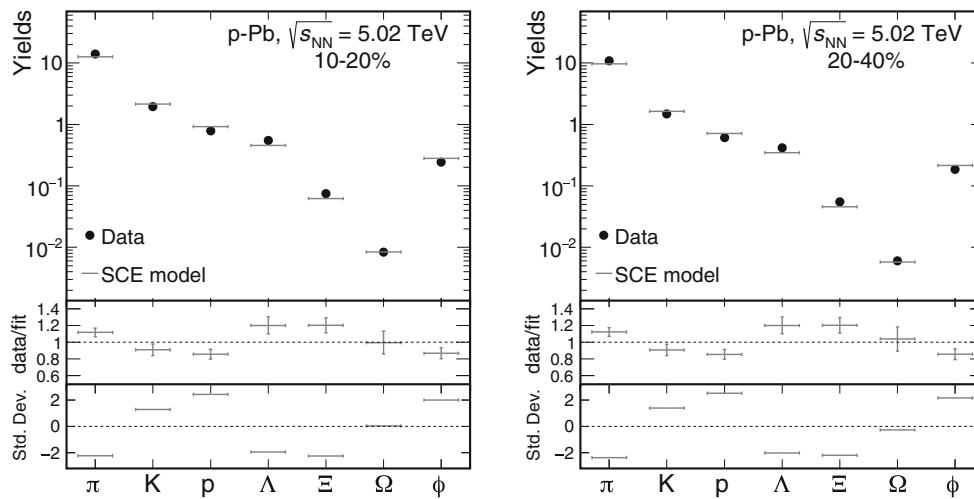


**Fig. 3** Comparison of data with fits for the 10–20 and the 20–40% centrality bins

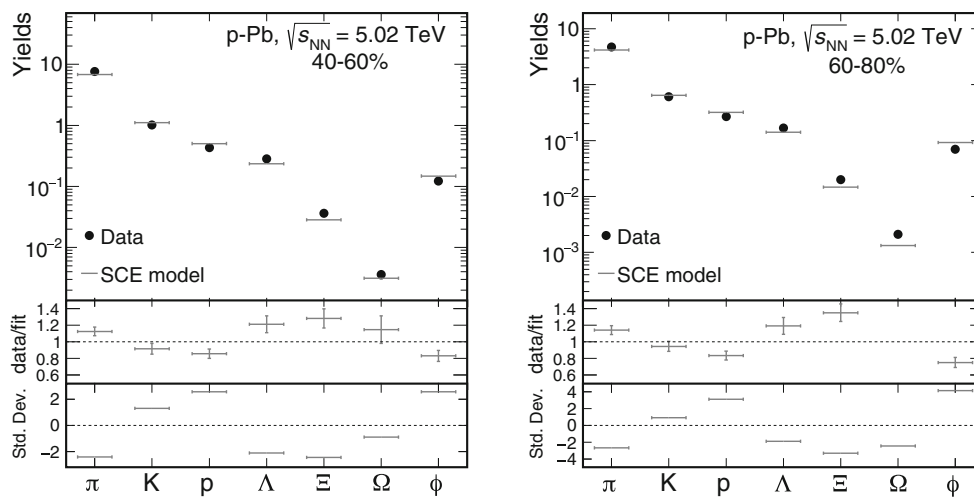


**Fig. 4** Comparison of data with fits for 40–60 and the 60–80% centrality bins. Note that in the centrality bin 60–80% the  $\Omega$  has a Data/Fit ratio of 1.58 which no longer fits on the plot

logarithmic scale easily hides the quality of the fits, we also show in the middle of the figures the ratio of the experimental data to the thermal model fit. In the lowest part of the figures we show the standard deviation for each particle, calculated in the standard way as Std. Dev.

$$\text{Std. Dev} \equiv (\text{Experimental value} - \text{Fit})/\text{Error}.$$

There are no very outstanding deviations from the thermal model fits. In particular, the  $\phi$  yield is reproduced reasonably well.

In Fig. 2 we present our results for the two most central multiplicity bins, i.e. 0–5 and 5–10%.

The pattern observed for the bins with the highest multiplicity reproduces itself for the next two bins i.e. 10–20 and 20–40% as shown in Fig. 3. The deviations from the thermal model are very similar to the previous ones. In particular, the yield of  $\phi$  mesons is again reasonably well reproduced. This

confirms the use of the strangeness non-equilibrium factor  $\gamma_s$ . The use of a different correlation radius for the strangeness suppression would not affect the  $\phi$  meson since it has net zero strangeness.

All yields are compatible with the thermal model description within two standard deviations. The next multiplicity bins are shown in Fig. 4. The left-hand side is consistent with the results shown in Figs. 2 and 3. The right-hand pane is a peripheral one corresponding to 60–80% centrality and shows the discrepancies with the thermal model fits. Especially there are clear deviations for the  $\Xi$  and  $\Omega$  baryons. The  $\phi$  is reasonably well described.

The largest deviations appear for the most peripheral collisions, 80–100%, and are shown in Fig. 5. Especially the values for data/fit are very high for the  $\Xi$  baryon at 2.45 and for the  $\Omega$  it is 4.6.

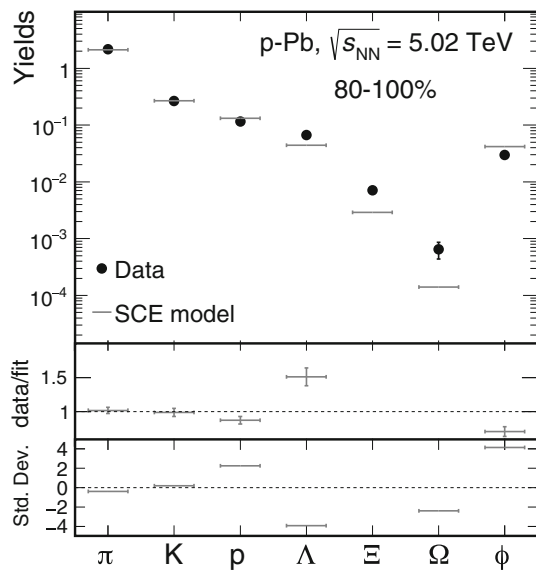


**Fig. 5** Comparison of data with fits for the most peripheral collisions. The lower part of the figure shows the standard deviation. The standard deviation for the  $\Xi$  is 5.5. While the ratios data/fit for the  $\Xi$  and  $\Omega$  are 2.45 and 4.6 respectively

To summarize the results obtained above we show the chemical freeze-out temperature  $T_{ch}$  and the corresponding radius  $R$  as a function of charged particle multiplicity in Fig. 6. The values of  $T_{ch}$  are remarkably independent of multiplicity except for the most peripheral bin. The radius determined from the yields fixes the normalization of the yields and shows a steady increase with the centrality of the collision. The more particles there are in the final state, the larger the radius and, correspondingly, the volume of the system. It should be noted that the volume increases linearly with the multiplicity. This indicates that the density of the fireball remains constant.

The values of the strangeness non-equilibrium factor  $\gamma_s$  are shown on Fig. 7. It can be seen that  $\gamma_s$  is very slowly

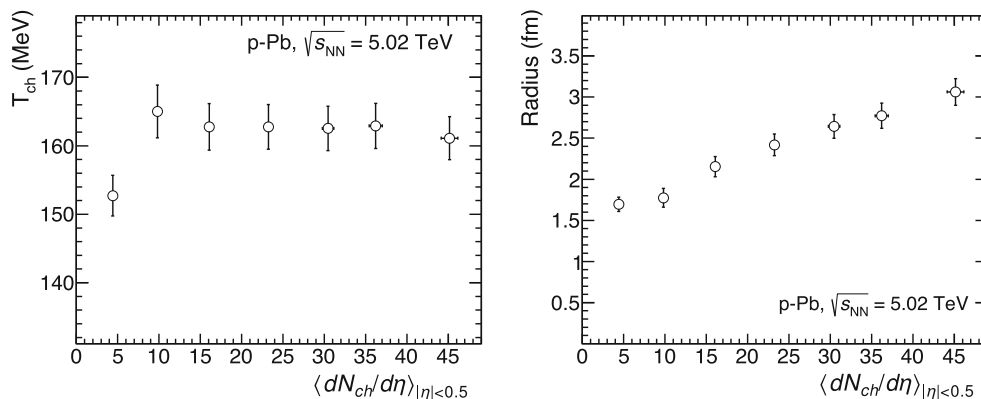


**Fig. 6** The temperature (left pane) and the radius (right pane) at chemical freeze-out as a function of charged particle multiplicity  $\langle dN_{ch}/d\eta \rangle_{|\eta|<0.5}$

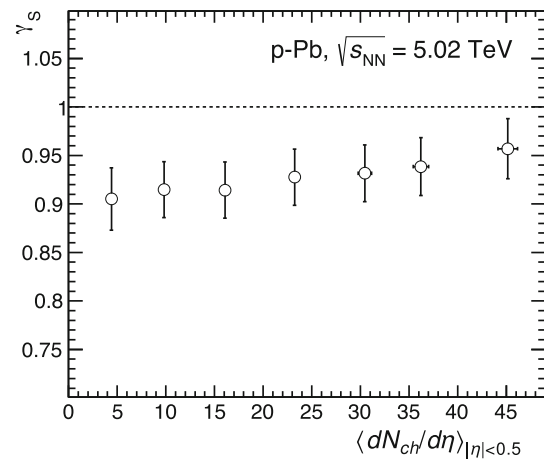


**Fig. 7** Values of the strangeness non-equilibrium factor  $\gamma_s$  as a function of the charged particle multiplicity  $\langle dN_{ch}/d\eta \rangle_{|\eta|<0.5}$

increasing with multiplicity, starting from a value of about 0.9 for the most peripheral collision reaching about 0.96 for the bin with the highest multiplicity. This shows that the system is very close to chemical equilibrium, the largest deviation being about 10%. Again, being so close to chemical equilibrium is a remarkable property of the fireball produced.

Apart from the most peripheral collisions, the chemical freeze-out temperature shows a remarkable consistency for all multiplicity classes. This shows that the final state hadrons are consistent with being produced in a single fireball having a temperature slightly about 160 MeV. The best fits are achieved for the most central collisions, the worst fits are for the two most peripheral bins. This is quantitatively reflected in the values of the  $\chi^2$  shown in Table 1.

The information presented above is summarized in Table II below. In addition the values of  $\chi^2$  are also listed. As can be seen by far the worst fits are obtained for the most peripheral collisions.

**Table 1** Chemical freeze-out temperature ( $T_{ch}$ ), radius ( $R$ ),  $\gamma_s$  and  $\chi^2/ndf$  of the fits for various multiplicity classes

Centrality (%)	$T_{ch}$ (MeV)	$R$ (fm)	$\gamma_s$	$\chi^2/ndf$
0–5	$161.10 \pm 3.10$	$3.06 \pm 0.16$	$0.96 \pm 0.031$	23.38/4
5–10	$162.93 \pm 3.30$	$2.77 \pm 0.15$	$0.94 \pm 0.030$	26.52/4
10–20	$162.53 \pm 3.23$	$2.64 \pm 0.14$	$0.93 \pm 0.029$	25.44/4
20–40	$162.75 \pm 3.03$	$2.42 \pm 0.13$	$0.93 \pm 0.037$	27.52/4
40–60	$160.48 \pm 3.37$	$2.22 \pm 0.12$	$0.91 \pm 0.029$	20.07/4
60–80	$165.00 \pm 3.78$	$1.77 \pm 0.11$	$0.91 \pm 0.029$	55.40/4
80–100	$152.72 \pm 2.96$	$1.69 \pm 0.09$	$0.90 \pm 0.032$	74.35/4

## 5 Conclusions

The fireball being produced in  $p$ - $Pb$  collisions has simple properties, it is close to full chemical equilibrium, the temperature is independent of the multiplicity in the final state and the radius increases smoothly which is to be expected for a system that increases with the multiplicity in the final state.

It is remarkable that the system is always close to full chemical equilibrium with  $\gamma_s$  never below 0.9 even for the most peripheral bins. The chemical freeze-out temperature is also remarkably constant, except (again) for the most peripheral bin. The radius decreases when going to more peripheral collisions, a feature which is to be expected.

Fits to  $pp$  collisions have recently been made [26] as a function of the multiplicity of charged particles in the event. It was shown that for the highest multiplicities the thermal model works very well and that a grand canonical description becomes valid.

For such a simple model based on only three parameters it is not surprising that a perfect agreement is not always reached, this can be clearly seen in the underestimation of the pion yield and the overestimate of the proton one. This indicates that the thermal model as presented here is, in our opinion, a very good first order description of the particle composition but that it is open to further improvements.

Some questions about this approach have been raised recently, e.g.:

- what is the effect of an incomplete list of hadronic resonances [27–30]?
- are there separate freeze-out temperature for strange particles [31,32]?
- is the theoretical description complete [33]?

The first question has to be answered by new experimental results on hadronic resonances. The latter two cases naturally lead to the introduction of new extra parameters which reduce the simplicity of the model.

In conclusion, in this paper we have performed an analysis of the particle composition in  $p$ - $Pb$  collisions at 5.02 TeV

using the thermal model. This model provides a good description of the hadronic yields. The largest deviations occurring for the most peripheral collisions. The chemical freeze-out temperature is independent of centrality  $T_{ch} = 162 \pm 3$  MeV, except for the lowest multiplicity bin, this value is consistent with values obtained in  $Pb$ - $Pb$  collisions. The value of the strangeness non-equilibrium factor  $\gamma_s$  is slowly increasing with multiplicity from 0.9 to 0.96, i.e. it is always very close to full chemical equilibrium.

**Acknowledgements** The authors acknowledge numerous useful discussions with J. Schukraft, B. Hippolyte and K. Redlich. One of us (J.C.) gratefully thanks the National Research Foundation of South Africa for financial support. N.S. acknowledges the support of SERB Ramanujan Fellowship (D.O. No. SB/S2/RJN- 269084/2015) of the Department of Science and Technology of India. L.K. acknowledges the support of the SERB grant No. ECR/2016/000109 of the Department of Science and Technology of India.

**Open Access** This article is distributed under the terms of the Creative Commons Attribution 4.0 International License (<http://creativecommons.org/licenses/by/4.0/>), which permits unrestricted use, distribution, and reproduction in any medium, provided you give appropriate credit to the original author(s) and the source, provide a link to the Creative Commons license, and indicate if changes were made. Funded by SCOAP<sup>3</sup>.

## References

1. M. Lorenz, (HADES), Nucl. Phys. A **967**, 27 (2017)
2. L. Adamczyk, et al. (STAR), Phys. Rev. C **96**(4), 044904 (2017). [arXiv:1701.07065](https://arxiv.org/abs/1701.07065)
3. M. Floris (ALICE), J. Phys. Conf. Ser. **668**(1), 012013 (2016)
4. W. Heisenberg, Z. Phys. **126**(6), 569 (1949)
5. E. Fermi, Phys. Rev. **92**, 452 (1953)
6. R. Hagedorn, Nuovo Cim. Suppl. **3**, 147 (1965)
7. B.B. Abelev et al., (ALICE). Phys. Lett. B **728**, 25 (2014). [arXiv:1307.6796](https://arxiv.org/abs/1307.6796)
8. J. Adam, et al., (ALICE), Phys. Lett. B **758**, 389 (2016). [arXiv:1512.07227](https://arxiv.org/abs/1512.07227)
9. J. Adam, et al., (ALICE), Eur. Phys. J. C **76**(5), 245 (2016). [arXiv:1601.07868](https://arxiv.org/abs/1601.07868)
10. V. Vislavicius, A. Kalweit (2016), [arXiv:1610.03001](https://arxiv.org/abs/1610.03001) [nucl-ex]
11. A. Andronic, P. Braun-Munzinger, K. Redlich, et al., (2017). [arXiv:1710.09425](https://arxiv.org/abs/1710.09425) [nucl-th]
12. F. Becattini, M. Bleicher, J. Steinheimer, et al. (2017). [arXiv:1712.03748](https://arxiv.org/abs/1712.03748) [hep-ph]

13. J. Cleymans, B. Kampfer, S. Wheaton, Phys. Rev. **C65**, 027901 (2002)/ [arXiv:nucl-th/0110035](#)
14. C. Patrignani, et al., (Particle Data Group), Chin. Phys. C **40**(10), 100001 (2016)
15. J. Cleymans, In *Proceedings, 3rd International Conference on Physics and astrophysics of quark-gluon plasma (ICPA-QGP '97)*, pp. 55–64 (1998). [arXiv:nucl-th/9704046](#)
16. W. Broniowski, W. Florkowski, Phys. Rev. Lett **87**, 272302 (2001). [arXiv:nucl-th/0106050](#)
17. S. V. Akkelin, P. Braun-Munzinger, Yu M Sinyukov, Nucl. Phys **A710**, 439 (2002). [arXiv:nucl-th/0111050](#)
18. J.D. Bjorken, Phys. Rev. D **27**, 140 (1983)
19. R. Hagedorn, K. Redlich, Z. Phys. C **27**, 541 (1985)
20. J. Cleymans, K. Redlich, E. Suhonen, Z. Phys. C **51**, 137 (1991)
21. P. Braun-Munzinger, J. Cleymans, H. Oeschler et al., Nucl. Phys. A **697**, 902 (2002). [arXiv:hep-ph/0106066](#)
22. J. Cleymans, H. Oeschler, K. Redlich, Phys. Rev. C **59**, 1663 (1999). [arXiv:nucl-th/9809027](#)
23. S. Hamieh, K. Redlich, A. Tounsi, Phys. Lett. B **486**, 61 (2000). [arXiv:hep-ph/0006024](#)
24. J. Letessier, A. Tounsi, U.W. Heinz et al., Phys. Rev. D **51**, 3408 (1995). [arXiv:hep-ph/9212210](#)
25. S. Wheaton, J. Cleymans, M. Hauer, Comput. Phys. Commun. **180**, 84 (2009). [arXiv:hep-ph/0407174](#)
26. N. Sharma, J. Cleymans, B. Hippolyte (2018). [arXiv:1803.05409](#) [hep-ph]
27. A. Bazavov et al., Phys. Rev. Lett. **113**(7), 072001 (2014). [arXiv:1404.6511](#)
28. P. Alba et al., Phys. Rev. D **96**(3), 034517 (2017). [arXiv:1702.01113](#)
29. P. Alba, W. Alberico, R. Bellwied et al., Phys. Lett. B **738**, 305 (2014). [arXiv:1403.4903](#)
30. M. Bluhm, P. Alba, W. Alberico et al., Nucl. Phys. A **929**, 157 (2014). [arXiv:1306.6188](#)
31. S. Chatterjee, A.K. Dash, B. Mohanty, J. Phys. **G44**(10), 105106 (2017). [arXiv:1608.00643](#)
32. R. Bellwied, In *17th International Conference on Strangeness in Quark Matter (SQM 2017) Utrecht, the Netherlands, July 10–15, 2017* (2017). [arXiv:1711.00514](#)
33. V. Vovchenko, M.I. Gorenstein, H. Stoecker, Phys. Rev. Lett. **118**(18), 182301 (2017). [arXiv:1609.03975](#)